

Spectral solar irradiance, atmospheric component and its relation with the production of photovoltaic current

Graciela M. Salum^{1,2}, Olga Vilela³, Manoel Pedrosa^{3,4}, Javier Cruceño² and Rubén D. Piacentini^{2,5}

¹Scholl of Physic Sciences and Nanotechnology, Yachay Tech, Urcuquí, Ecuador

²Instituto de Física Rosario (CONICET-Univ. Nacional de Rosario), Rosario, Argentina

³ Nuclear Energy Department, Federal University of Pernambuco, Recife - PE (Brazil)

⁴ Instituto Federal de Educação, Ciência e Tecnologia de Pernambuco, Pesqueira, Brazil

⁵LESyC, IMAE, Univ. Nacional de Rosario, Rosario, Argentina

Abstract

We present results of spectral solar irradiance measured by a high quality double-monochromator spectroradiometer in different seasons at the Astronomical Observatory of Rosario, Argentina. Since measures were done in the UV and visible ranges, we extended the measurements using the SMARTS model. Also, the model is applied to extend the analysis of spectral solar irradiance for Recife (Brazil) and Urcuquí (Ecuador). The maximum photovoltaic current for different solar cells (monolayer and multilayer) was derived using spectral irradiance associated to quantum efficiency of the PV cells. At 5th May 2013, the calculated photovoltaic currents were: 33.47 mA/cm² (mono-Si); 25.42 mA/cm² (poly-Si); 18.52 mA/cm² (CdTe); 12.28 mA/cm² (multilayer cell). The sensitivity of each cell technology to different atmospheric components (e.g., aerosols, water vapour, ozone) is also shown.

Keywords: *spectral, solar irradiance, photovoltaic cells, quantum efficiency*

1. Introduction

Solar spectral irradiance is one of the variables most difficult to be measured due to the requirement of high quality instruments (spectroradiometers) with a periodic calibration and to the modification of the atmospheric components (gases and suspended particles, aerosols and clouds) that can vary rapidly. Even the Sun position changes more than 1° in only some minutes. Consequently, special care needs to be taken in order to measure solar spectral irradiances in outdoor conditions. In the present work we present these measurements done in the Astronomical Observatory of Rosario, Argentina (32.95° S, 60.68°W, 25 m asl) in different months of the year, with an OL756 portable UV-Vis spectroradiometer Optronics, a double monochromator, in the 280-400 nm and 400-750 nm (UV and visible) ranges.

We are mainly interested in the correlation of these spectral data with the photovoltaic (PV) current produced by (mono- and multi-) layer solar cells. Since usually these cells have quantum efficiencies that go up to the IR wavelength range, we used an extension of the data considering the SMARTS (Gueymard, 1995) algorithm. Currents (per unit area of the incident radiation) in the range of 10.02-38.3 mA/cm² can be obtained, depending on the maximum efficiency, the place and the spectral range of the considered cell. Theoretical analysis of the maximum limiting efficiencies has been obtained by Araújo and Martí (1994) with values of 40.8% for optimum single gap devices and of 86.8% for infinite number of gaps.

The significance of solar photovoltaic as a renewable energy source has been highlighted by Razykov et al. (2011) indicating that the PV market is growing at an annual rate of 35-40%. Also the reduction to around 1 year in the time at which the solar cells equals the energy consumed for its production to the generated energy

and the minimization of the environmental impact of a solar power plant has been discussed by Piacentini et al. (2013).

2. Results and discussions

2.1 Spectral solar irradiances

It was measured spectral solar irradiances at the Rosario Astronomical Observatory, Argentina, from 290 to 420 nm during clear sky days (with cloud coverage $\leq 25\%$) on horizontal plane, employing an Optronics OL756 spectroradiometer of the Institute of Physics Rosario (CONICET-National University of Rosario). This high quality instrument is a double monochromator (eliminating in this way the straylight effect that produces false signal at wavelength less than about 300 nm) with calibration lamp. In order to extend the wavelength range in the visible and infrared (IR) parts of the spectrum, we employed the SMARTS algorithm (Gueymard, 1995) for the model calculation of the solar spectral irradiance corresponding to the same day and hour of measurement.

The solar spectral global irradiance was modelled through SMARTS model using satellite data. The air temperature at 10 m, relative humidity, total column precipitable water and surface albedo were obtained from the SSE/NASA, the ozone total column with OMI/NASA and AOD_{550m} (aerosol optical depth to 550 nm) with MODIS-Aqua Deep Blue.

The ozone and aerosol components were modified in order to have a very good match between model calculation and spectral measurements in the UV range. In order to adjust the model to measurement was used as a criterion "the area adjusted". This means, to find a small percentage difference between the areas of the irradiances. For May 03, 2013, the percentage difference was 0.12% and in the case of December 28, 2011 was 0.54%. In Fig. 1, it can be seen the measurement superimposed to modelling.

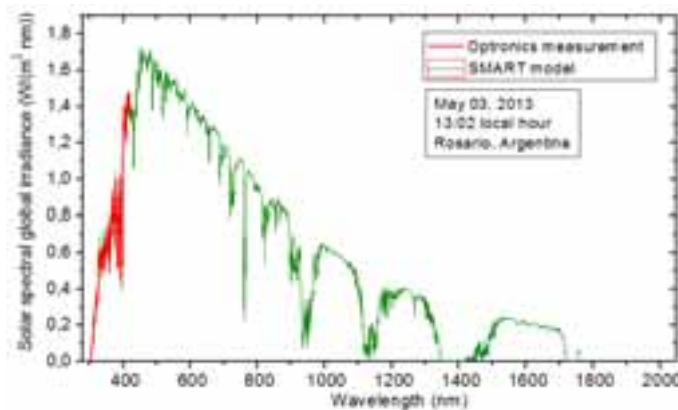


Figure 1: Solar spectral global irradiance incident on a horizontal surface for Rosario, Argentina, in May 03, 2013. The red line represents the Optronics measurement and the green line represents the SMART model result.

In Figure 2 (left), we display the solar spectral global irradiance for the days: December 28, 2011 at 13:03 local hour (=UT - 3); and May 05, 2013 at 13:02 local hour. The irradiances displayed in Figure 2 show the typical behavior of sun radiation in the UV-visible-IR ranges (see for example the reference spectrum of Gueymard, 1995), with strong absorption at certain particular wavelengths due to atmospheric gases.

In the Urququi case, since a lack of measurements, it was modelled the solar spectral global irradiance through SMARTS model using the same satellite data bases.

The selected days were: September 24 and July 21 because they are the days with the minimum (1.1°) and

maximum (80.6°) solar zenith angle respectively for the place, see Fig.2 (middle). The reason for the election site is based in the altitude of the Urcuquí, since this place is located at 2320 masl (meters above the sea level). Also, Urcuquí has a low aerosol optical depth (0.046 in September and 0.137 in July). The middle of Figure 2, we shows the solar spectral global irradiance calculated with the SMARTS for Urcuquí.

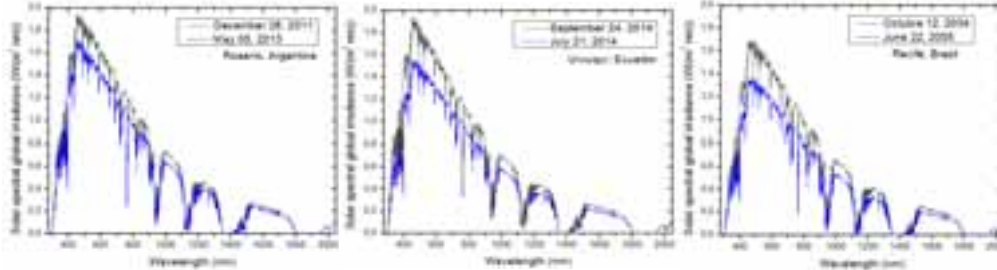


Figure 2: Solar spectral global irradiance incident on a horizontal surface for Rosario, Argentina (left), Urcuquí, Ecuador (middle) and Recife, Brazil (right). In the case of Rosario, the model was used to extrapolate the measurements and in the cases of Urcuqui and Recife all data was modeling.

Also, for Recife there is a lack of calibrated measurements, then it was modelled the solar spectral global irradiances for two day through SMARTS model using the same satellite data base. It was modeled the following days: June 22, 2005 and October 12, 2004 (see Fig.2, right).

2.2 Spectral quantum efficiency

The figure 3 shows the quantum efficiency for different types of solar cells. Quantum efficiency refers to the efficiency with which photons that reaches the cell is able to generate collectable carriers. It depends on the absorption characteristics of the solar cell. The upper limit wavelength for each type of cell is determined by the energy gap of the materials that composes the solar cell. Photons with energy lower than this limit is not absorbed.

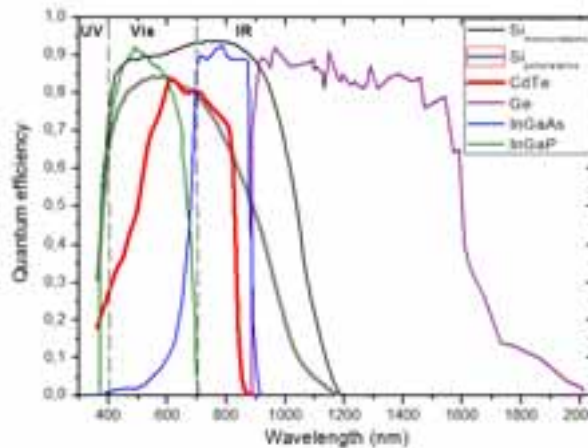


Figure 3: External quantum efficiency of different solar cells as function of wavelength.

The quantum efficiency of InGaAs, InGaP and Ge presented in Fig. 3 were obtained directly from the datasheet of a manufacturer of multijunction solar cells. The curves presented for the other materials (Fig. 3) were obtained using the relationship between quantum efficiency (QE) and spectral response (SR), presented by Field (1997) in equation (1).

$$QE = \frac{hc}{\lambda q} SR \quad (\text{eq. 1})$$

were q is the absolute value of electron charge, λ is the wavelength, h is the Planck constant, and c the the speed of light in vacuum.

3. 2.3 Spectral and total surface density photovoltaic current

The photovoltaic current (per unit area) is produced in the solar cell by the interaction of solar photons with the material exposed to the Sun. This can be described mathematically through the following equations (2 to 4):

$$I_{FV,A} = \int_{\lambda_2}^{\lambda_1} \varphi \cdot \varepsilon_{\lambda} \cdot \Delta\lambda \quad (\text{eq. 2})$$

$$\varphi = \frac{I(\lambda,t)}{E_f} \cdot e^{-} \quad (\text{eq. 3})$$

$$E_f = \frac{h \cdot c}{\lambda} \quad (\text{eq. 4})$$

being φ the maximum spectral surface density photovoltaic current, e^{-} the electron charge, $h =$ Planck's constant, ε_{λ} the solar cell external quantum efficiency, $\Delta\lambda = \lambda_2 - \lambda_1$ the wavelength interval which is defined from the external quantum efficiency wavelength range of each solar cell, and E_f is a photon energy.

One of the purposes of studying the photogenerated current is the possibility to analyze the efficiency of the solar cell to capture solar radiation in different regions of South America. For example, Hau-Vei et al. (2014) presented a hybrid design of the GaAs combined with colloidal quantum dots, achieving a power conversion efficiency as high as 24.65% compared with traditional GaAs-based devices and current densities until approximately 23 mA/cm². Also, Mohammed et al (2013) presented a model for simulation of the enhancement of the photogenerated current por PN silicon photodetectors with impurities.

Figure 4 shows the maximum spectral surface density photovoltaic current, the particular quantum efficiency and the weighted value with external quantum efficiency for different solar cells for a typical clear sky day (May 5, 2012 in Rosario) around solar noon. We also indicate in the same figure the integral value of this weighted value ($\varphi \cdot \varepsilon_{\lambda}$). The corresponding values of the surface density photovoltaic current are summarized in Table 1 showing that the maximum current corresponds to the mono-Si and the minimum one to InGaAs, in all cases.

Table 1: Integrated weighted surface density photovoltaic current (iFV,A) for different days of the year and for monolayer and polylayer solar cells. Also, the ratio between the maximum and minimum current values and the mean (with its standard deviation) values are included.

Date (local hour = UT-3)	Place	iFV,A (mA/cm ²) for different solar cells							Ratio max/min	Mean value (standard deviation)
		InGaP	InGaAs	Ge	mono-Si	poly-Si	CdTe			
28/12/2011 (13:02)	Rosario Argentina	17.09	13.97	18.68	38.30	29.04	21.15	2.13	23.7 (8.4)	
05/05/2012 (13:02)	Rosario Argentina	14.82	12.28	17.86	33.47	25.42	18.52	2.73	21.9 (11.1)	
24/09/2014 (13:00)	Urcuquí Ecuador	16.81	13.67	18.8	37.61	28.49	20.68	2.75	22.7 (8.8)	
21/07/2014 (13:00)	Urcuquí Ecuador	13.68	11.33	15.70	30.96	23.96	17.01	2.73	18.8 (7.3)	
22/06/2005 (11:30)	Recife Brazil	12.10	10.02	12.91	27.13	20.59	15.10	2.71	16.3 (6.4)	
12/10/2005 (11:20)	Recife Brazil	15.03	12.48	16.54	33.87	25.67	18.75	2.71	20.4 (8.0)	

Araújo and Martí (1994) obtained an optimum photogenerated current of 56.09 mA/cm² with their model, while Razykov et al. (2011) determined a short-circuit current density of 42.2 mA/cm², with an efficiency of 24.7%. Steudel et al. (2012) presented a short-circuit current density of 17.94 mA/cm² in a CdTe solar cell for an air mass of 1.5. As it can be seen in Table 1, our calculations gave a range of 15.10 to 21.15 mA/cm² for the same type of solar cells with air mass between 1 and 1.54

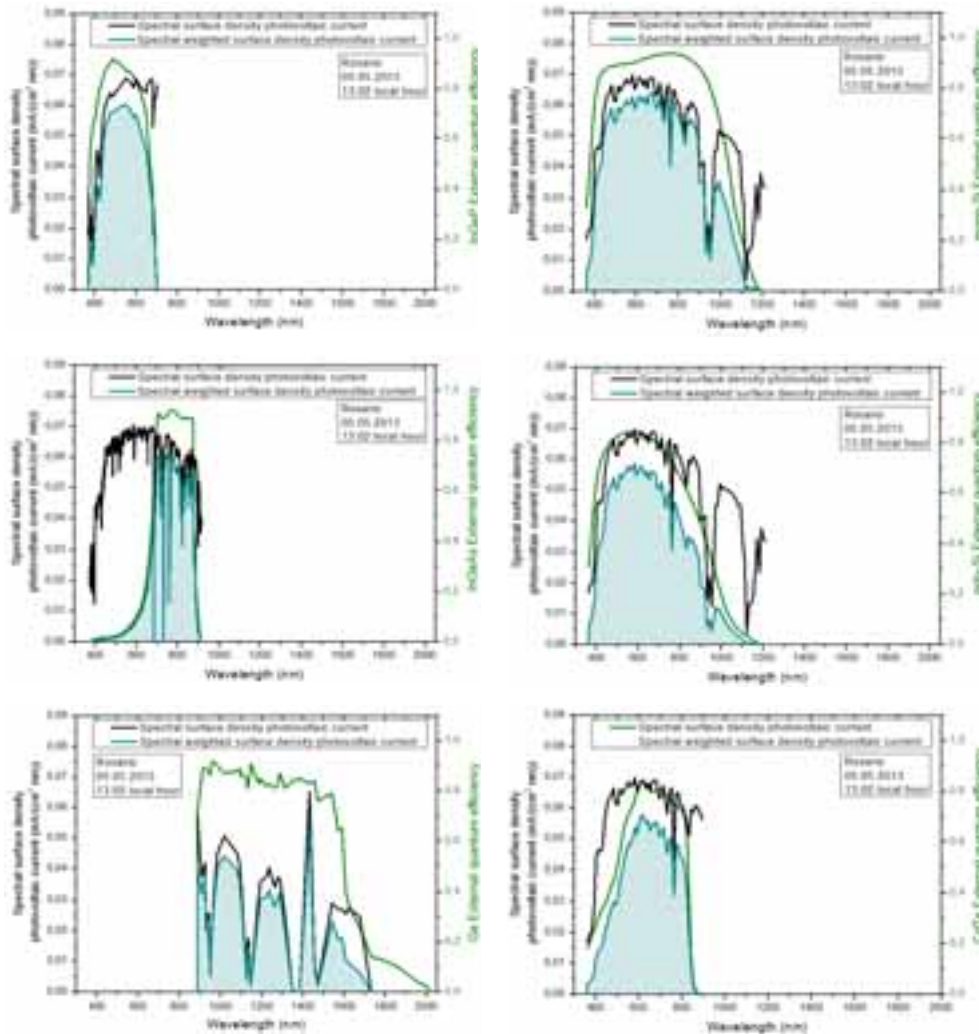


Figure 4: Spectral surface density photovoltaic current (black line) and weighted (cyan shading area) with external quantum efficiency (green line) for different solar cells determined for solar spectral irradiance measured the day May 5, 2013 at 13:02 local hour at the Astronomical Observatory of Rosario, Argentina. The integrated weighted surface density photovoltaic current is also given.

4. 2.4 Sensibility analysis

As a general criteria for the analysis of the influence of each atmospheric component on the surface density photovoltaic current, first it was analyzed if there is a significant wavelength superposition of the external quantum efficiencies and the atmospheric transmittance of given gases or aerosol. From Figure 5 and considering the criteria described before, it can be deduced qualitatively that the water vapor amount in the atmosphere influences mainly in the Ge solar cell. The total column ozone and the aerosols have more impact over the InGaP cells while they have less impact on Ge cells.

It was calculated the sensibility for three different parameters with the data of Rosario in December 28, 2011. The corresponding results of the sensitivity of the different atmospheric component variation on surface density photovoltaic current ($i_{FV,A}$) is given in Table 2. They confirm the initial hypothesis. To build the Table 2, each parameter (ozone, aerosol and water precipitation) were changed in ten percent and it was calculated the percentage change of the resulting surface density photovoltaic current.

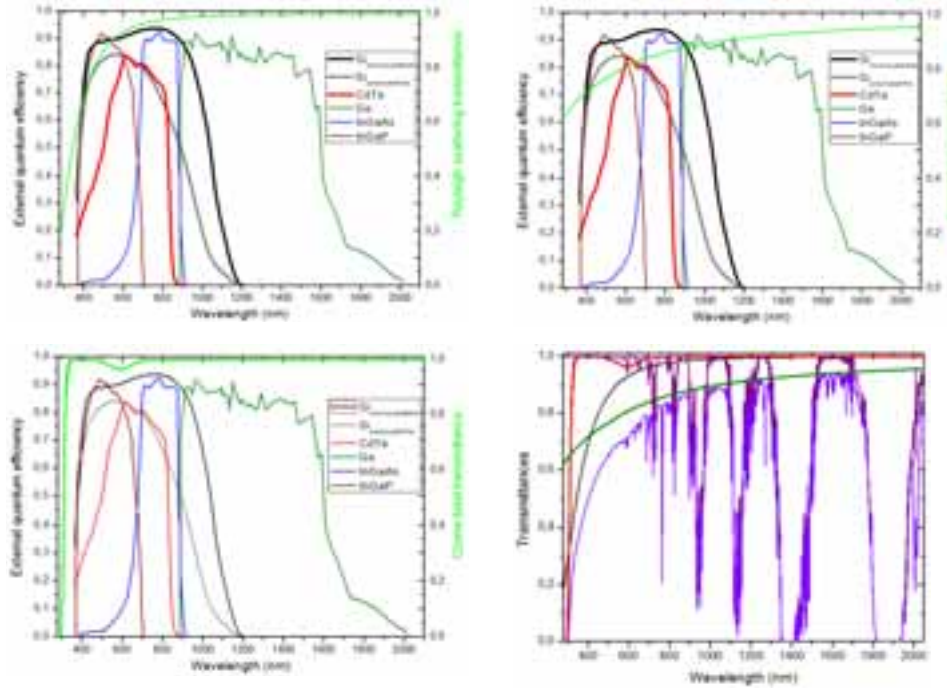


Figure 5: Transmittances and its relationship with the different external quantum efficiency of solar cells. Top left: Rayleigh scattering transmittance. Top Right: aerosol total transmittance. Bottom left: ozone total transmittance. Bottom right: All transmittance at December 28, 2011 in Rosario: ozone total (red line), Rayleigh scattering (black line), aerosol (green line), water vapor (purple line) and total (violet line) transmittances.

Table 2: Analysis of the sensitivity ($\Delta i_{FV,A} \%$) of atmospheric component variation on surface density photovoltaic current ($i_{FV,A}$) for Rosario in December 28, 2011. Top: with change of total column ozone. Middle: with change of AOD_{550nm} . Bottom: with change of precipitable water.

Parameters		$i_{FV,A}$ (mA/cm ²) for different solar cells					
		InGaP	InGaAs	Ge	mono-Si	poly-Si	CdTe
Total column ozone (DU)	265.5	17.09	13.97	18.68	38.30	29.04	21.15
	292.05	17.06	13.96	18.68	38.26	29.00	21.12
$\Delta i_{FV,A} \%$	10	0.176	0.071	0	0.104	0.138	0.142

Parameters		$i_{FV,A}$ (mA/cm ²) for different solar cells					
		InGaP	InGaAs	Ge	mono-Si	poly-Si	CdTe
AOD_{550nm}	0.2325	17.09	13.97	18.68	38.30	29.04	21.15
	0.25575	17.02	13.94	18.65	38.19	28.95	21.09
$\Delta i_{FV,A} \%$	10	0.410	0.215	0.161	0.287	0.310	0.284

Parameters		$i_{FV,A}$ (mA/cm ²) for different solar cells					
		InGaP	InGaAs	Ge	mono-Si	poly-Si	CdTe

Precipitable water (cm)	2.71	17.09	13.97	18.68	38.30	29.04	21.15
	2.98	17.09	13.97	18.68	38.30	29.04	21.15
$\Delta i_{FV,A} \%$	10	0	0	0	0	0	0

In the last case, a change of ten percentage in the precipitable water value did not produce a change in the surface density photovoltaic current.

5. 3. Conclusions and future perspectives

The main results and conclusions are:

-Spectral solar irradiance has been measured and modelled for Rosario (Argentina), Urcuquí (Ecuador) and Recife (Brazil), at different seasons permitting to have a wide wavelength range, in order to calculate photovoltaic current.

-Spectral and total surface density photovoltaic current shows a range between 10.02mA/cm² (for June 22, 2005, in Recife) and 38.3mA/cm² (for December 28, 2011, in Rosario).

-Sensibility analysis of atmospheric components of the total surface density photovoltaic current, shows that a change of ten percentage of the total column ozone and the same change in the AOD_{550nm} produces the largest decrease in the current solar cells of InGaP, in both cases, and smallest in the Ge solar cells. A change of ten percent in the precipitable water do not produce a change in a current of any solar cell.

6. Acknowledgements

The authors like to acknowledge the following institutions: CONICET, Argentina, Yachay Tech University, CNPq - Brazil and persons Fernando Fernández and Joel Gornati.

7. References

- Araújo, G.L., Martí, A., 1994. Absolute limiting efficiencies for photovoltaic energy conversion. *Solar Energy Materials and Solar Cells*. 33, 213-240.
- Field, H., 1997. Solar cell spectral response measurement errors related to spectral bandwidth and chopped light waveform. 26th IEEE Photovoltaic Specialists Conference. Anaheim, California. 1997
- Gueymard, C.A., 1995. SMARTS, A Simple Model of the Atmospheric Radiative Transfer of Sunshine: Algorithms and Performance Assessment. Technical Report No. FSEC-PF-270-95. Cocoa, FL: Florida Solar Energy Center.
- Hau-Vei, H., Chien-Chung, L., Yu-Lin, T., Hsin-Chu, C., Kuo-Ju, C., Yun-Ling, Y., Wen-Yi, L., Hao-Chung, K., Peichen Y., 2014. Highly Efficient Hybrid GaAs Solar Cell Based on Colloidal-Quantum-Dot-Sensitization. *Scientific Reports*. 4 : 5734 | DOI: 10.1038/srep05734
- Mohammed, W.F., Humoody, M.A., Al-Tikriti, M.N., 2013. Simulation of photogenerated current of PN silicon photodetector enhanced by impurity photovoltaic effect. *Renewable and Sustainable Energy Reviews* 26, 408–413
- Piacentini, R.D., Schmidt J., Budini N., Vega M., Giandoménico E., Feldman S., Buitrago R., 2013. Photovoltaic materials and solar power plant optimization design in relation to its environmental impact. En el libro: *Energy Book Series - Volume # 1: "Materials and processes for energy: communicating current research and technological developments"*, 103-113.

Salum et al. / SWC 2015/ ISES Conference Proceedings (2015)

Razykov, T.M., Ferekides, C.S., Morel, D., Stefanakos, E., Ullal, H.S., Upadhyaya, H.M., 2011. Solar photovoltaic electricity: Current status and future prospects. *Solar Energy*. 85 (8) 1580–1608

Stedel, F., Dyrba, M., Schweizer, S., 2012. Fluorescent borate glass enhances cadmium telluride solar cells. *Proc SPIE*, DOI: 10.1117/2.120126.004235